Journal of Manufacturing Processes 25 (2017) 220–226

Contents lists available at ScienceDirect

Journal of Manufacturing Processes

journal homepage: www.elsevier.com/locate/manpro

Technical Paper

Microstructure characteristic and mechanical property of pulsed laser lap-welded nickel-based superalloy and stainless steel

Siyu Zhou, Dongsheng Chai, Jingling Yu, Guangyi Ma, Dongjiang Wu*

Key Laboratory for Precision and Non-traditional Machining Technology of Ministry of Education, Dalian University of Technology, Dalian, 116024, China

ARTICLE INFO

Article history:
Received 26 July 2016
Received in revised form
13 November 2016
Accepted 17 November 2016

Keywords:
Pulsed laser
Dissimilar welding
Element distribution
Mechanical property

ABSTRACT

To evaluate the effects of pulsed laser welding on the microstructure characteristics and mechanical properties of nickel-based superalloy (C-276) and austenitic stainless steel (304) lap-welded joint, the analyses of morphology, microstructure, phase structure, element distribution, tensile–shear strength and microhardness were carried out. The results indicated the unmixed zone was found at the interface between the weld metal (WM) and 304. A small number of inter-dendritic precipitates were also found, and the precipitates were most probably p or μ phases. Compared with the phase structure in C-276, the dominated phase structure in the WM was also austenite phase, however, the lattice constant was reduced due to the decrease of Ni, Mo and W content. The macro-element distribution was inhomogeneous in the WM due to the rapid cooling rate in pulsed laser welding, and the element transition region adjacent to C-276 was wider than that adjacent to 304. The fracture mode of lap-welded joint in tensile–shear test was tensile fracture, and the tensile strength was decreased by 17% compared with that of C-276. The microhardness value in the WM was not lower than that in the base metals.

1. Introduction

Nickel-based superalloy (C-276) and austenitic stainless steel (304) are extensively employed in the fabrication of components in nuclear plants and chemical industries because of their high mechanical properties and corrosion resistance [1–4]. Dissimilar welding is inevitably applied for the joining of the two alloys in these situations. The nickel-based alloy and austenitic stainless steel components are generally fabricated using conventional welding processes, such as the gas tungsten arc welding (GTAW). Researches were primarily focused on the selection of welding wire and welding parameters in a butt configuration. Banovic et al. [5] investigated the influence of filler metal feedrate on the dilution and microsegregation in the dissimilar welding of super austenitic stainless steel (AL-6XN) and two nickel-based alloys (Inconel 625 and Inconel 622). Wang et al. [6] studied the microstructure and microhardness at fusion boundary in the 316 stainless steel/Inconel 182 dissimilar welding. Naffakh et al. [7] conducted the welding of Inconel 657 nickel–chromium superalloy to 310 austenitic stainless steel using four types of filler materials, and they concluded that the Inconel a filler wire offered the best compromise for the dissimilar weld joint. Hosseini et al. [8] used three types of filler materials in the Inconel 617/310 austenitic stainless steel dissimilar welding, finding that the mechanical properties of weld joint with the Inconel 617 filler material were much better than those with other fillers.

Compared with the conventional welding processes, laser welding has a number of key advantages, including the finer grain and lower residual stress, which improves welding quality [9–11]. Especially, during the pulsed laser welding, the cooling rate is much faster than that during the continuous wave laser welding, which could further decrease the trend of the formation of brittle phase. There are a few literatures on the laser dissimilar welding of nickel-based alloy and austenitic stainless steel. For example, Li et al. [12] carried out the study on the microstructure and properties of Inconel 625 and 304 stainless steel butt weld using high-power CO_2 continuous wave laser. The pulsed laser welding of C-276 and 304 in an overlap configuration was rarely reported. However, this C-276/304 lap-welded joint was widely used, for example, in the seal welding of pump can (C-276 sheet with 0.5 mm thickness) and end cap (304 with a much larger thickness) in the nuclear reactor coolant pump. Conventional argon arc welding process has been used in the sealing welding of pump can and end cap. However, because of the unstable welding process, a large number of precipitates, coarse grain and large welding deformation in argon arc welding, the sealing weld joint tended to craze during the high-pressure leak detection, and it was difficult to ensure the sealing reliability of weld joint. Hence, pulsed laser welding process was

* Corresponding author.
E-mail address: djwu@dlut.edu.cn (D. Wu).

http://dx.doi.org/10.1016/j.jmapro.2016.11.010
1526-6125/

Table 1
Normal compositions of nickel-based superalloy C-276 and 304 stainless steel (wt.%).

Materials	Ni	Fe	Cr	Mo	W	Co	Mn	C	Si	P	S	V
304	8–10.5	Bal.	18–20	–	–	–	≤2	≤0.08	≤1.0	≤0.035	≤0.03	–
C-276	Bal.	4–7	14–16	15–17	3–4.5	≤2.5	≤1.0	≤0.01	≤0.08	≤0.04	≤0.03	≤0.035

first introduced in the C-276/304 dissimilar lap-welding to overcome the deficiencies in argon arc welding.

In this paper, the systematic studies of morphology, microstructure, phase structure, element distribution, tensile–shear strength and microhardness of lap-welded joint were carried out. The effect of pulsed laser welding on the microstructure characteristics and the mechanical properties of C-276/304 dissimilar lap-welded joint was investigated.

2. Experimental procedures

The base metals used in this research were nickel-based superalloy (C-276) sheet with a thickness of 0.5 mm and austenite stainless steel (304) sheet with a thickness of 2.0 mm. The base metals mainly consisted of equixed grains with a size of 20 μm–50 μm. The chemical compositions of the C-276 and 304 base metals are given in Table 1, in weight percent. They were cut to the size of $40 \times 100\ mm^2$. C-276 was placed on 304 in an overlap configuration. A fixture was used to provide a good contact between the upper and lower sheets. The laser source was a Nd:YAG laser with a maximum mean power of 500 W. Pure argon gas was used as the shielding gas, and the gas flow rate was 12 L/min. The laser welding parameters included the pulse energy, pulse duration, pulse repetition, welding velocity and defocus distance. In order to obtain an excellent weld joint with flat surface, no obvious defects and large connection width, the optimized welding parameters were selected as 4.0 J, 6 ms, 30 Hz, 150 mm/min and 0 mm. The laser beam focused on the upper surface of welding sample was approximately 0.6 mm in diameter.

For metallographic examinations, the sample after laser processing was prepared from the cross-section of weld joint. The sample was prepared by grinding using SiC papers, followed by the final polishing with 1.5 μm diamond powder. The electrolytic etching in a reagent of 10% oxalic acid was used to examine the microstructures of the WM and C-276. The solution of 10 mL HNO_3 + 30 mL HCl was used as the etching reagent to examine microstructures of the 304 base metal and the interface between the WM and 304. The microstructure characteristic was observed by optical microscope (OM) and scanning electron microscope (SEM) equipped with an energy-dispersive X-ray spectrometer (EDS). Electron probe microanalysis (EPMA) was used to analyze the element distribution. The tensile–shear test was carried out to evaluate the mechanical properties of weld joint at room temperature with a constant travel speed of 5 mm/min. The tensile–shear sample is schematically shown in Fig. 1. Peak loads were extracted from the load displacement curve, and the failure mode was obtained from the failed samples. On the cross-section of weld joint, the vickers microhardness test was carried out in the horizontal direction (300 μm away from the weld centerline for the C-276 side and 100 μm for the 304 side) using a load of 50 g and dwell time of 15 s.

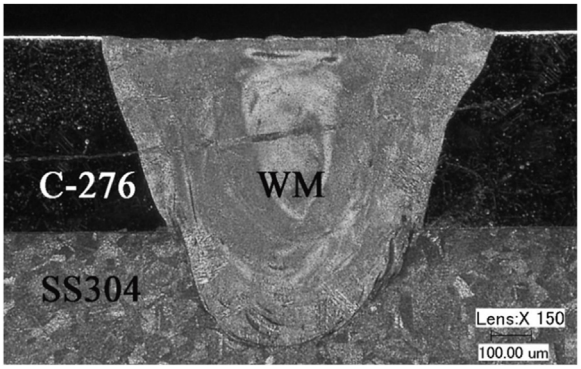

Fig. 2. Cross-section of the weld joint.

3. Results and discussion

3.1. Microstructure characteristics

Fig. 2 shows the cross-section morphology of dissimilar weld joint. The upper surface was flat, and there were no obvious defects such as crack or porosity being found in the WM. By measuring the melted areas of C-276 ($A_{C\text{-}276}$) and 304 (A_{304}), the geometrical dilution level of 304 base metal was defined as $D = A_{304}/(A_{304} + A_{C\text{-}276})$. The average element composition could be calculated as $C_{weld} = C_{304}D + C_{C\text{-}276}(1 - D)$ [13], where C_{weld}, C_{304}, and $C_{C\text{-}276}$ are the element compositions in the WM, 304 and C-276 respectively. The calculated element compositions of Ni, Fe, Cr and Mo are 47.01%, 20.97%, 17.36% and 12.27%, in weight percent. The average element compositions in the WM were also measured by EDS (the measured area is selected as 300 μm × 300 μm), and the measured concentrations (wt.%) of major elements Ni, Fe, Cr and Mo were 49.17%, 22.71%, 16.14% and 11.08%.

The interfacial microstructures between C-276, 304 and WM are represented in Fig. 3(a) and (b). The pulsed laser welding with low heat input enhances the rapid solidification. In addition, the thermal conductivities of base metals were large enough to accelerate the thermal conduction. Hence, the thermal accumulation near the WM was weakened, and no obvious HAZ were observed in both

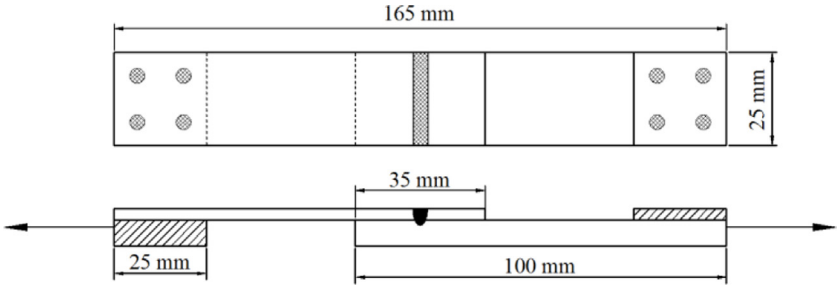

Fig. 1. A schematic of tensile–shear sample.